Supplement of

Effect of relative humidity on molecular composition of secondary organic aerosol from α-pinene ozonolysis

*Hao Luo[1,2,3‡], Yindong Guo[1,2‡], Hongru Shen[1,2], Dan Dan Huang[4], Yijun Zhang[1,2,3,5,6], Defeng Zhao[1,2,3,5,7]**

[1] Department of Atmospheric and Oceanic Sciences & Institute of Atmospheric Sciences, Fudan University, Shanghai, 200438, China

[2] Shanghai Frontiers Science Center of Atmosphere-Ocean Interaction, Fudan University, Shanghai, 200438, China.

[3] Shanghai Key Laboratory of Ocean-land-atmosphere Boundary Dynamics and Climate Change, Fudan University, Shanghai, 200438, China

[4] State Environmental Protection Key Laboratory of Formation and Prevention of Urban Air Pollution Complex, Shanghai Academy of Environment Sciences, Shanghai, 200233, China

[5] National Observations and Research Station for Wetland Ecosystems of the Yangtze Estuary, Fudan University, Shanghai, 200438, China

[6] Shanghai Institute of Pollution Control and Ecological Security, Shanghai, 200092, China

[7] Institute of Eco-Chongming (IEC), 20 Cuiniao Rd., Chongming, Shanghai, 202162, China.

‡ These authors contributed equally to this work.

CONTENT

THE ESTIMATED EQUILIBRATION TIMESCALES OF VAPOR-PARTICLE AND VAPOR-WALL PARTITIONING

The timescale of vapor-particle partitioning ($\tau_{v,p}$) refers to the partitioning of vapors directly condensing on particles, which can be quantified as follows [Huang et al.,2016; Seinfeld and Pandis., 2016]:

$$\tau_{v,p} = (2\pi N_p \bar{D}_p \mathcal{D}_g f(Kn, \alpha_p))^{-1};$$

where N_p and $\bar{D}_p$ are the total number concentration and number mean particle diameter of suspended particle, respectively; $\mathcal{D}_g$ means the gas-phase diffusion coefficient of a specific organic vapor; Kn is Knudsen number, which is equal to $2\lambda/D_p$; α_p is vapor accommodation coefficient on particles, and for α-pinene SOA, α_p ranges from 0.01-0.1 [Stanier et al., 2007; Saleh et al., 2013; Vaden et al., 2011]; $f(Kn, \alpha_p)$ denotes the correction factor for non-continuum diffusion and imperfect accommodation.

The timescale of vapor-wall equilibrium partitioning ($\tau_{v,w}$) represents the partitioning between the vapor deposited on the reactor wall and particle, which can be obtained as follows [Zhang et al., 2015]:

$$\tau_{v,w} = \frac{1}{(\frac{A}{V})(\frac{\alpha_w v/4}{1 + \pi\alpha_w \bar{v}/8(D_g K_e)^{1/2}})(1 + \frac{C^*}{C_w})}$$

where A, V, and K_e are the surface area, volume, and the coefficient of eddy diffusion of the reactor, respectively; $\bar{v}$ represents the species mean thermal speed. C^* means the mass saturation concentration of the vapor species, and C_w represents the mass concentration of absorbing organic material on the wall. α_w means the vapor accommodation coefficient on the reactor wall, which is related to both the mass transfer resistances at the vapor-wall interface and in the wall layer itself. The parameter α_w can be obtained according to the inverse dependence of α_w on C^*, which is similar to the treatment of vapor-particle partitioning.

53 FIGURE S1-S8

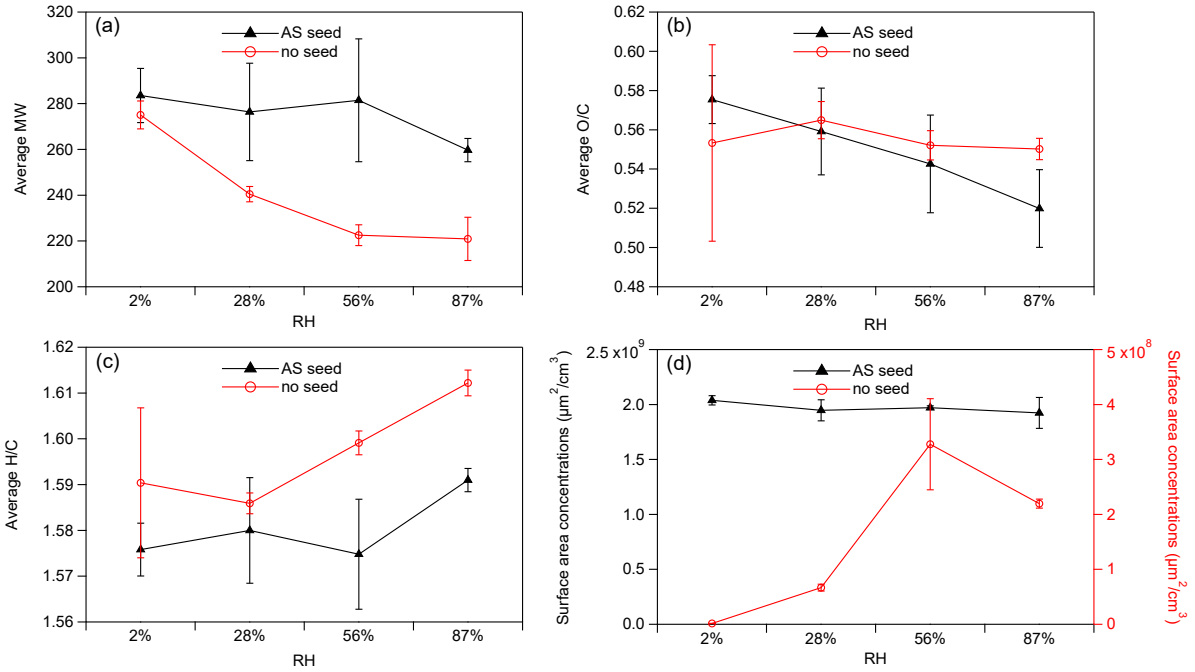

54

55 **Figure S1. The (a) average molecule weight (MW), (b) O:C, (c) H:C, and (d) surface area**
56 **concentrations in the absence and presence of AS seed under different RH.**

57

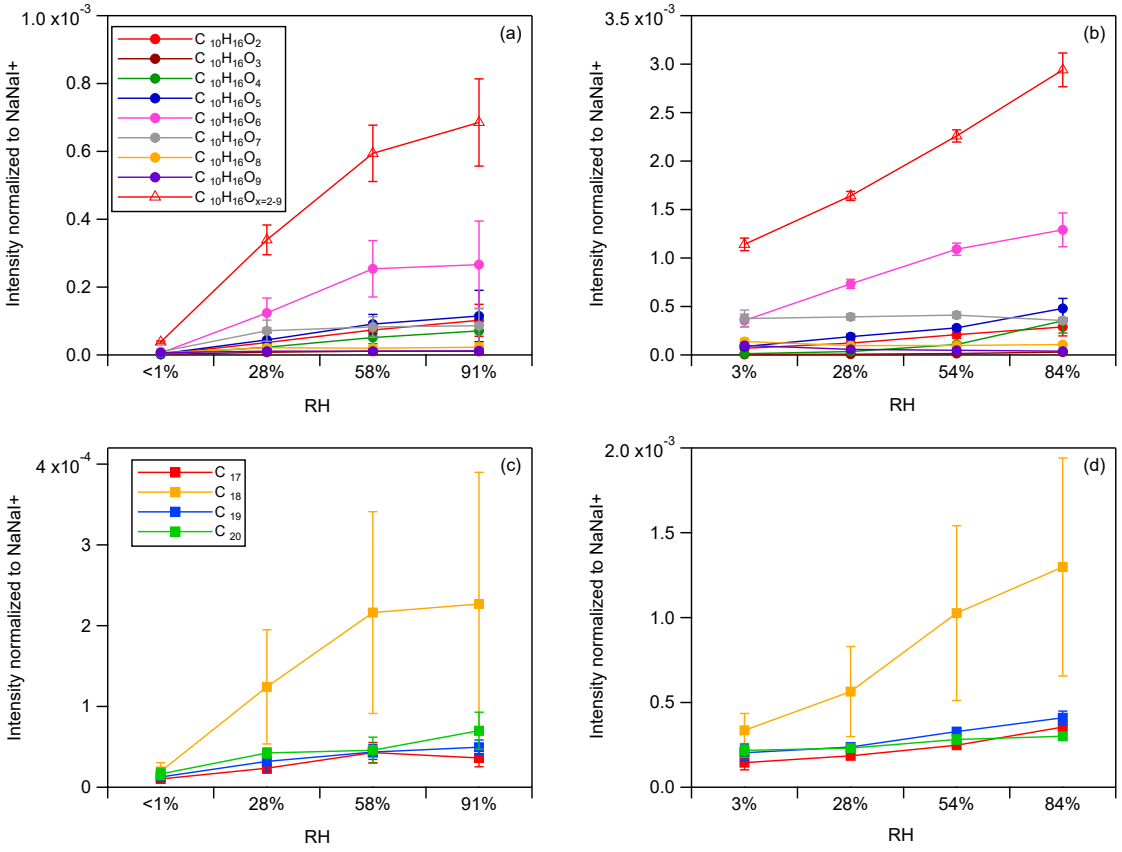

Figure S2 The absolute abundance of monomer ($C_{10}H_{16}O_x$, circle) and dimers (C_{17-20}, square) under RH ramp. (a)(c) without AS seed; (b)(d) with AS seed. Note that all intensity were normalized to $NaINa^+$, which is the stable ion source signal with the top intensity.

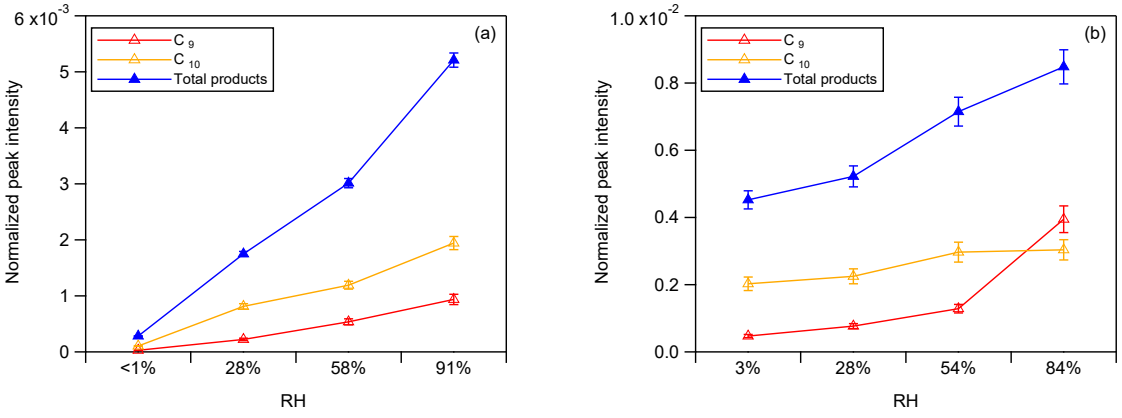

Figure S3. The absolute abundance of total C_9 and total products as a function of RH in the (a) absence and (b) presence of AS seed. Note that the peak intensity in mass spectra were normalized to the peak intensity of $NaINa^+$ (m/z 173), which is the most intensive peak from ion source.

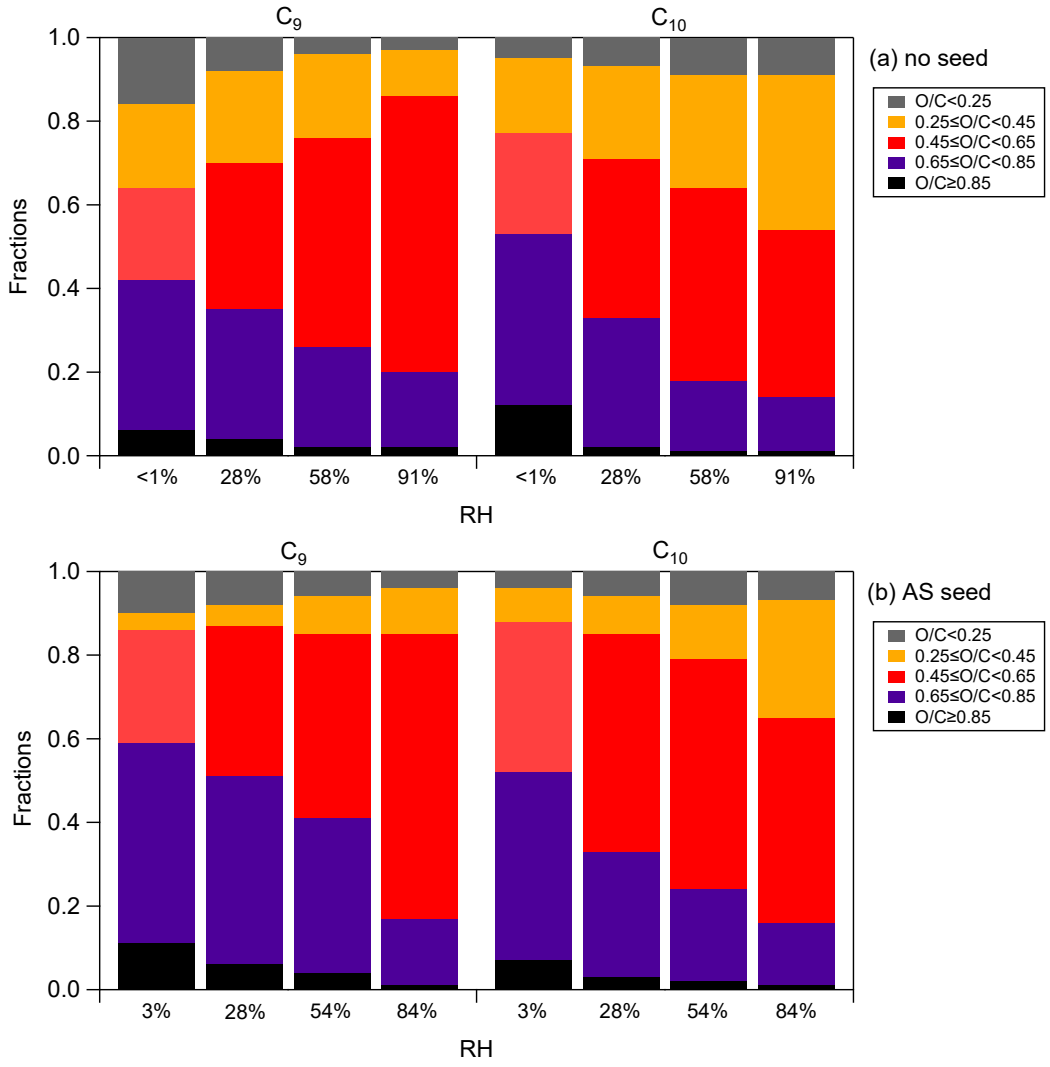

Figure S4. The fraction of C_9 and C_{10} monomers with different O/C ratios as a function of RH

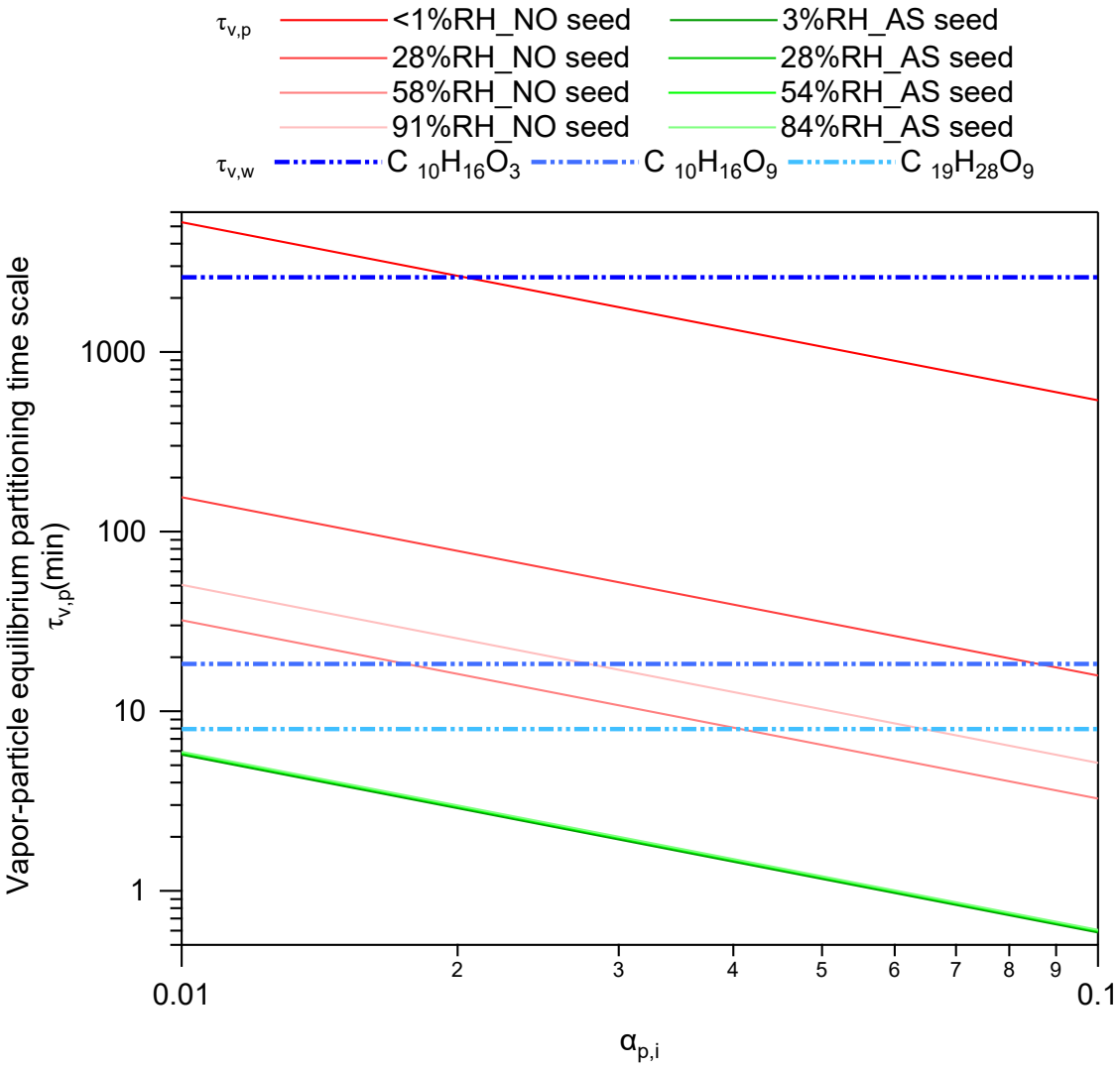

69

70 **Figure S5 The estimated vapor-particle ($\tau_{v,p}$) and vapor-wall equilibration timescale ($\tau_{v,w}$). Red**
71 **and green solid line represent vapor-particle equilibration time scale as function of vapor mass**
72 **accommodation coefficients on particle (α_p) in the absence and presence of AS seed conditions.**
73 **The blue dashed lines mean vapor-wall equilibration timescale of a representative SVOC**
74 **($C_{10}H_{16}O_3$, dark blue), LVOC ($C_{10}H_{16}O_9$, medium blue), and ELVOC ($C_{19}H_{28}O_9$, light blue).**

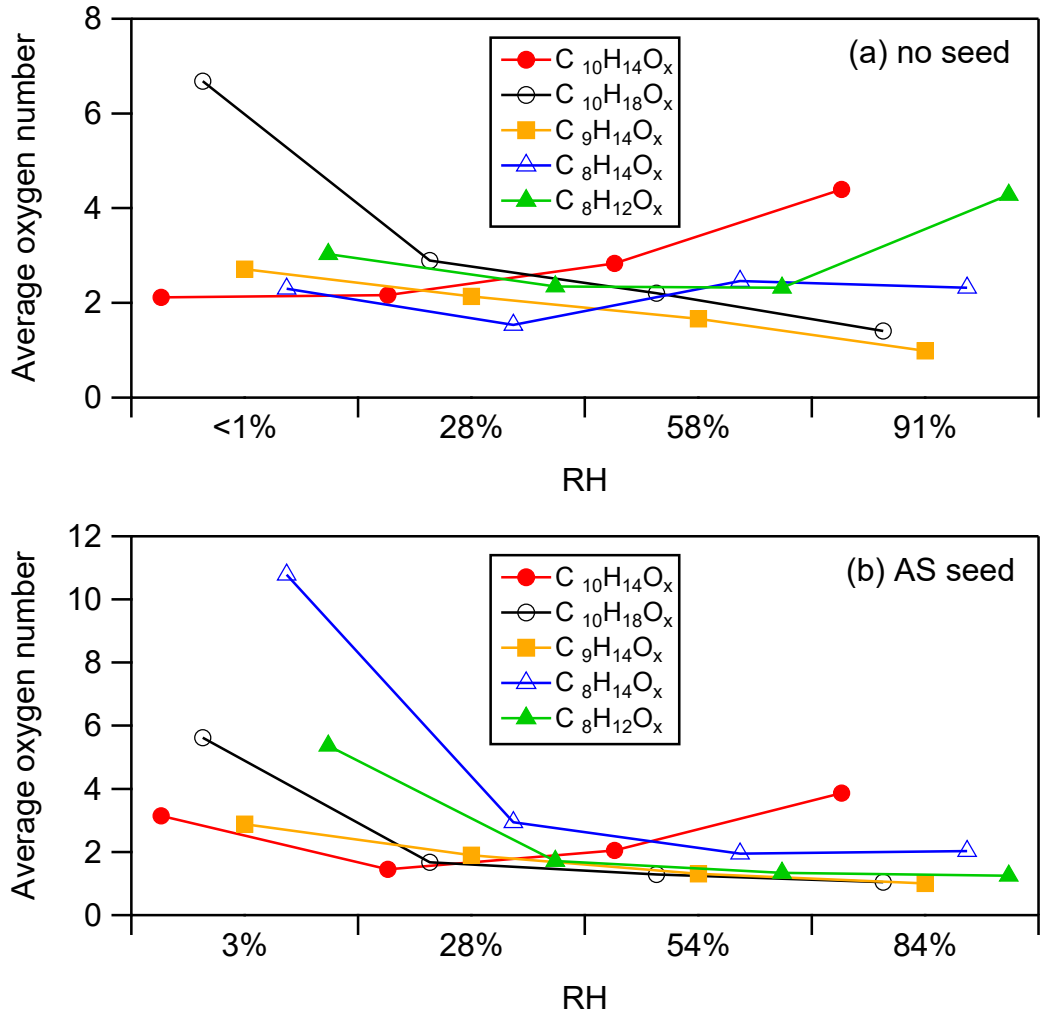

75

76 **Figure S6. The average oxygen number of monomer families under different RH in the (a)**
77 **absence and (b) presence of AS seed.**

78

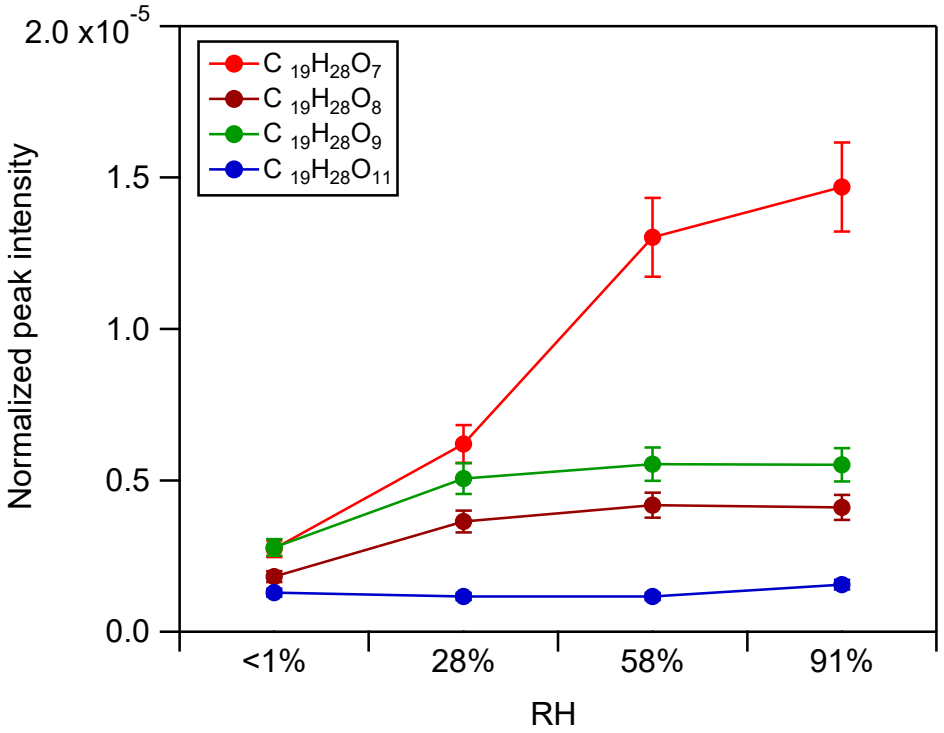

79

80 **Figure S7 The absolute abundance of $C_{19}H_{28}O_x$ in the absence of seed aerosol. Note that the peak**
81 **intensity in mass spectra were normalized to the peak intensity of $NaINa^+$ (m/z 173), which is**
82 **the most intensive peak from ion source.**

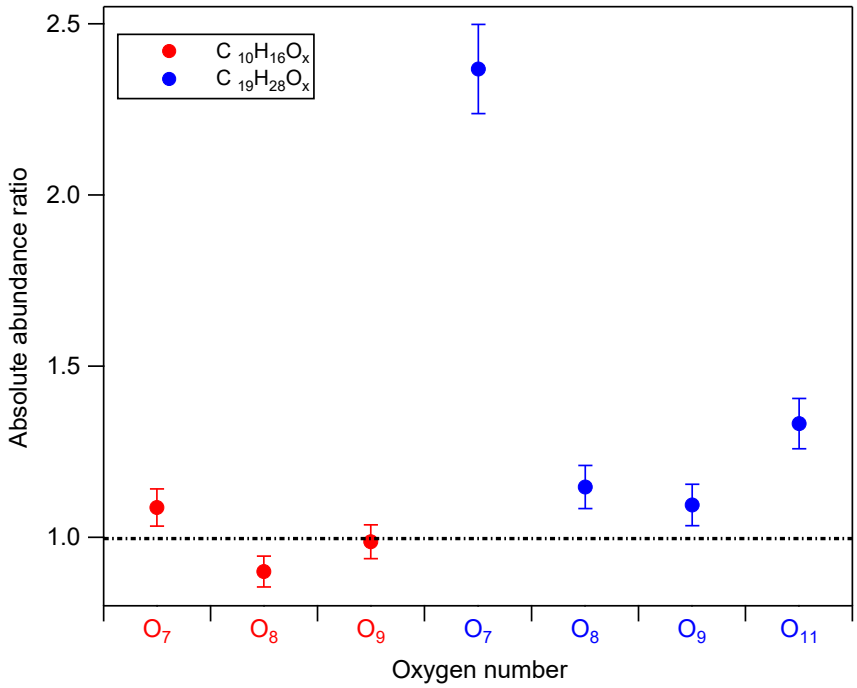

83

84 **Figure S8 The abundance ratio of $C_{10}H_{16}O_x$ (red) and $C_{19}H_{28}O_x$ (blue) at 91%RH and 28%RH in**
85 **the absence of AS seed.**

TABLE S1

Table S1 Experimental conditions in this study

NO.	AS seed	OH scavenger (2-propanol)	a-pinene concentrations (ppbv)	O_3 concentrations (ppbv)	Initial aerosol mass concentration (μg/m3)	Residence time (min)	Volume of flow tube (L)	Temperature (K)	RH(%)			
									RH1	RH2	RH3	RH4
1	×	√	161.0±9.0	480.0±20.5	<0.05	14.2	45.9	299.0	0	28	60	93
2	×	√	161.0±9.0	480.0±20.5	<0.05	15.0	45.9	298.0	0	28	57	90
3	×	√	161.0±9.0	480.0±20.5	<0.1	14.9	45.9	298.0	0	27	56	90
4	√	√	161.0±9.0	480.0±20.5	43.6±5.1	14.1	45.9	298.0	3	27	53	81
5	√	√	161.0±9.0	480.0±20.5	34.6±5.1	14.1	45.9	298.0	4	30	56	87
6	√	√	161.0±9.0	480.0±20.5	31.5±5.1	14.1	45.9	298.0	4	29	56	87

TABLE S2

Table S2 Identification of products molecular formula

m/Q	molecular formula
126.031	C6H6O3
126.068	C7H10O2
134.021	C4H6O5
142.062	C7H10O3
146.021	C5H6O5
146.057	C6H10O4
148.037	C5H8O5
148.073	C6H12O4
154.099	C9H14O2
156.078	C8H12O3
156.114	C9H16O2
158.057	C7H10O4
158.094	C8H14O3
164.032	C5H8O6
166.099	C10H14O2
168.114	C10H16O2
170.057	C8H10O4
170.094	C9H14O3
172.073	C8H12O4
172.109	C9H16O3
174.052	C7H10O5
174.089	C8H14O4
176.068	C7H12O5
182.094	C10H14O3
184.073	C9H12O4
184.109	C10H16O3
186.089	C9H14O4
186.125	C10H18O3
188.068	C8H12O5

188.104	C9H16O4
190.084	C8H14O5
198.089	C10H14O4
200.068	C9H12O5
200.104	C10H16O4
202.084	C9H14O5
202.12	C10H18O4
204.063	C8H12O6
204.099	C9H16O5
204.136	C10H20O4
206.078	C8H14O6
214.084	C10H14O5
216.099	C10H16O5
218.078	C9H14O6
218.115	C10H18O5
220.058	C8H12O7
220.094	C9H16O6
228.063	C10H12O6
228.099	C11H16O5
230.078	C10H14O6
232.094	C10H16O6
234.073	C9H14O7
234.11	C10H18O6
236.053	C8H12O8
236.089	C9H16O7
238.068	C8H14O8
246.073	C10H14O7
248.089	C10H16O7
250.068	C9H14O8
250.105	C10H18O7
252.048	C8H12O9
252.084	C9H16O8
254.063	C8H14O9
262.068	C10H14O8

264.084	C10H16O8
264.208	C17H28O2
270.219	C16H30O3
280.079	C10H16O9
280.203	C17H28O3
290.188	C18H26O3
290.224	C19H30O2
294.058	C10H14O10
294.131	C12H22O8
294.183	C17H26O4
294.219	C18H30O3
306.183	C18H26O4
306.219	C19H30O3
306.255	C20H34O2
310.177	C17H26O5
310.214	C18H30O4
312.193	C17H28O5
314.172	C16H26O6
314.245	C18H34O4
320.198	C19H28O4
322.177	C18H26O5
322.214	C19H30O4
322.25	C20H34O3
324.193	C18H28O5
324.23	C19H32O4
326.172	C17H26O6
326.209	C18H30O5
328.188	C17H28O6
334.214	C20H30O4
336.141	C14H24O9
336.178	C15H28O8
336.23	C20H32O4
338.172	C18H26O6
338.209	C19H30O5

340.152	C17H24O7
342.167	C17H26O7
342.204	C18H30O6
344.147	C16H24O8
344.183	C17H28O7
346.162	C16H26O8
352.188	C19H28O6
352.224	C20H32O5
353.232	C20H33O5
354.167	C18H26O7
354.204	C19H30O6
356.183	C18H28O7
358.162	C17H26O8
358.199	C18H30O7
360.178	C17H28O8
360.214	C18H32O7
364.173	C16H28O9
366.152	C15H26O10
366.204	C20H30O6
368.183	C19H28O7
368.219	C20H32O6
370.162	C18H26O8
370.199	C19H30O7
372.193	C22H28O5
374.157	C17H26O9
374.194	C18H30O8
376.173	C17H28O9
376.188	C21H28O6
380.168	C16H28O10
384.178	C19H28O8
384.214	C20H32O7
386.194	C19H30O8
386.23	C20H34O7
388.246	C20H36O7

398.194	C20H30O8
398.23	C21H34O7
400.173	C19H28O9
400.209	C20H32O8
402.167	C22H26O7
402.225	C20H34O8
414.188	C20H30O9
416.204	C20H32O9
430.183	C20H30O10
432.163	C19H28O11
432.199	C20H32O10
462.137	C19H26O13
462.173	C20H30O12
592.148	C20H32O20

TABLE S3

Table S3 T-test results of the difference between dimer fractions at different RH in the presence and absence of AS seed

AS seed	(3±1)%/ (28±2)%	(3±1)%/ (54±2)%	(3±1)%/ (84±3)%	(28±2)%/ (54±2)%	(28±2)%/ (84±3)%	(54±2)%/ (84±3)%
t	4.62	3.11	2.14	-0.45	-0.48	-0.45
P	0.00	0.00	0.04	0.66	0.64	0.66
No seed	(<1)%/ (28±1)%	(<1)%/ (58±2)%	(<1)%/ (91±2)%	(28±1)%/ (58±2)%	(28±1)%/ (91±2)%	(58±2)%/ (91±2)%
t	7.42	8.03	8.73	3.31	3.94	2.56
P	0.00	0.00	0.00	0.00	0.00	0.01

References:

Seinfeld, J. H. and Pandis, S. N.: Atmospheric chemistry and physics : from air pollution to climate change (3nd Edn.), John Wiley & Sons, Inc., Hoboken, NJ, 2016.

Stanier, C. O., R. K. Pathak, and S. Pandis (2007), Measurements of the volatility of aerosols from alpha-pinene ozonolysis, Environ. Sci. Technol., 41(8), 2756–2763.

Saleh, R., Donahue, N. M., and Robinson, A. L.: Time scales for gas-particle partitioning equilibration of secondary organic aerosol formed from alpha-pinene ozonolysis, Environ. Sci. Technol., 47, 5588–5594.

Vaden, T. D., D. Imre, J. Beranek, M. Shrivastava, and A. Zelenyuk (2011), Evaporation kinetics and phase of laboratory and ambient secondary organic aerosol, Proc. Natl. Acad. Sci. U. S. A., 108: 2190–2195,

Zhang, X., Schwantes, R. H., McVay, R. C., Lignell, H., Coggon, M. M., Flagan, R. C., and Seinfeld, J. H. (2015), Vapor wall deposition in Teflon chambers, Atmos. Chem. Phys., 15, 4197–4214.